Acoustic resistance properties of new γ-austenitic alloys of the Fe–Cr–Mn system in the temperature range 5–325 K

Yu.A. Semerenko, L.N. Pal'-Val' and L.V. Skibina

B.I. Verkin Physical-Technical Institute of Low temperatures, National Academy of Sciences of Ukraine, prosp. Lenina 47, 61103 Khar'kov, Ukraine

The temperature dependences of vibration decrement, dynamic Young's modulus and electroresistivity of the stable austenitic $Fe_{100-x-y}Cr_xMn_y$ alloy (x = 5–10%, y = 30–40%, N, C, S, P < 0.1%, Si < 0.3%) in the temperature range 5–325 K, are investigated. This alloy is promising for atomic industry, aerospace and cryogenic engineering.

1. Introduction

The development of modern cryogenic, atomic and chemical engineering is closely linked with the increasing demands on the weldability of corrosion-resisting stainless steels. Advances in materials science make it possible to use, in addition to austenitic stainless steels, also high-strength austenitic–martensitic and martensitic steels [1, 2]. Nevertheless, the interest in stable austenitic steels is still very strong as a result of the combination of relatively high strength with high plasticity. The conventional method of ensuring the stability of the austenitic structure is to increase the nickel content. This greatly increases the price and weight of metal components and, consequently, the steels of this type are not promising for use in aerospace industry. The application of traditional chromium–nickel alloys in the atomic industry is restricted because of the formation of the long life β-radioactive nickel isotope under the effect of neutron radiation. The promising direction of solving this problem is the application of chromium–manganese stainless steels, efficiently alloyed with nickel or without nickel, because chromium and manganese do not produce long-life radioactive isotopes. In the construction of cryogenic devices, it is important to utilise the superconductivity effect, and the non-magnetic properties of the structural materials also become very important.

A promising direction for the development of readily available cheap high-strength

and lighter stainless steels, satisfying the requirements of atomic, cryogenic and aerospace engineering, is the utilisation of the austenitic range of the Fe–Cr–Mn system. However, there are at least two serious problems in the development of the steels. The first problem is the metastability of austenite and, consequently, the reduction of the plasticity and toughness of these steels. To ensure the stability of austenite, it is necessary to alloy the material with nitrogen and nickel in large quantities and this is undesirable. Another problem is the decrease of the plasticity and toughness of the steels alloyed with large amounts of chromium as a result of the presence of carbides and nitrides in the structure of quenched and tempered austenite and also the formation of precipitates at the grain boundaries.

Therefore, the main task in the development of nickel-free γ-austenitic steels of the Fe–Cr–Mn system is the selection of the optimum ratio of the main components at the minimum carbon content (less than 0.1%) and the addition of specific amount of nitrogen – the interstitial element – which increases corrosion resistance, stabilises and hardens the γ-austenitic phase, but reduces plasticity and toughness and also increases the stress concentration sensitivity at low temperatures.

In [3, 4] investigations were carried out into the distribution of plasticity and toughness at cryogenic temperatures in nickel-free austenitic steels with 0–15% Cr and 20–50% Mn and less than 0.1% C and N. The resultant relationships were used to determine the optimum composition of the stable austenitic alloy: $Fe_{100-x-y}Cr_xMn_y$ ($x = 5–10\%$, $y = 30–40\%$, N ≈ 0.05%). The steels with this composition are characterised by high plasticity, strength and low susceptibility to corrosion in media with a slight corrosion effect (in the atmospheric conditions), and they can be produced in industrial air electric arc furnaces. The alloys with 5–10% Cr and 40–45% Mn are also characterised by high plasticity and impact toughness but they are not resistant to corrosion and are difficult to produce in industrial electric arc furnaces and, consequently, do not represent promising materials.

The investigations of the phase composition, strength margin and plasticity of the most promising $Fe_{100-x-y}Cr_xMn_y$ alloys ($x = 5–10\%$, $y = 30–40\%$, N ≈ 0.05%) in a wide temperature range were carried out in [3, 4]. The present study is concerned with the investigations of previously not investigated acoustic and resistance properties of these alloys.

2. Experimental specimens and procedure

The temperature dependences of decrement δ, the dynamic Young modulus E and electrical resistance ρ of new $Fe_{100-x-y}Cr_xMn_y$ alloys ($x = 5, 10$; $y = 30, 35, 40$) promising for use in cryogenic and atomic engineering have been investigated in the temperature range 5–325 K. The content of the principal impurities: C, N, S, P < 0.1% and Si < 0.3%. Specimens of two types were investigated: 1) cylindrical bars produced from cold-drawn wire with a diameter of ≅1 mm; 2)

rectangular bars with the size of $3 \times 2 \times 25$ mm and $4 \times 0.3 \times 22$ mm thin sheets taken from thick cold-rolled blanks. The specimens had the γ-austenite structure (Fig. 1) produced by annealing for 1 h at 1273 K and followed by quenching in water. The specimens, containing 30% Mn and 5–10% Cr, were situated in the boundary region of the phase diagram and can contain a certain amount (no more than 2%) of the ε-martensite phase whose fraction can increase under the effect of plastic deformation.

The temperature in the process of acoustic and resistance measurements were measured with the accuracy of 50 µK using a Cu–Constantan thermocouple, an AsGa thermometer and a resistance heater. The temperature variation rate was $\cong 1$ K/min.
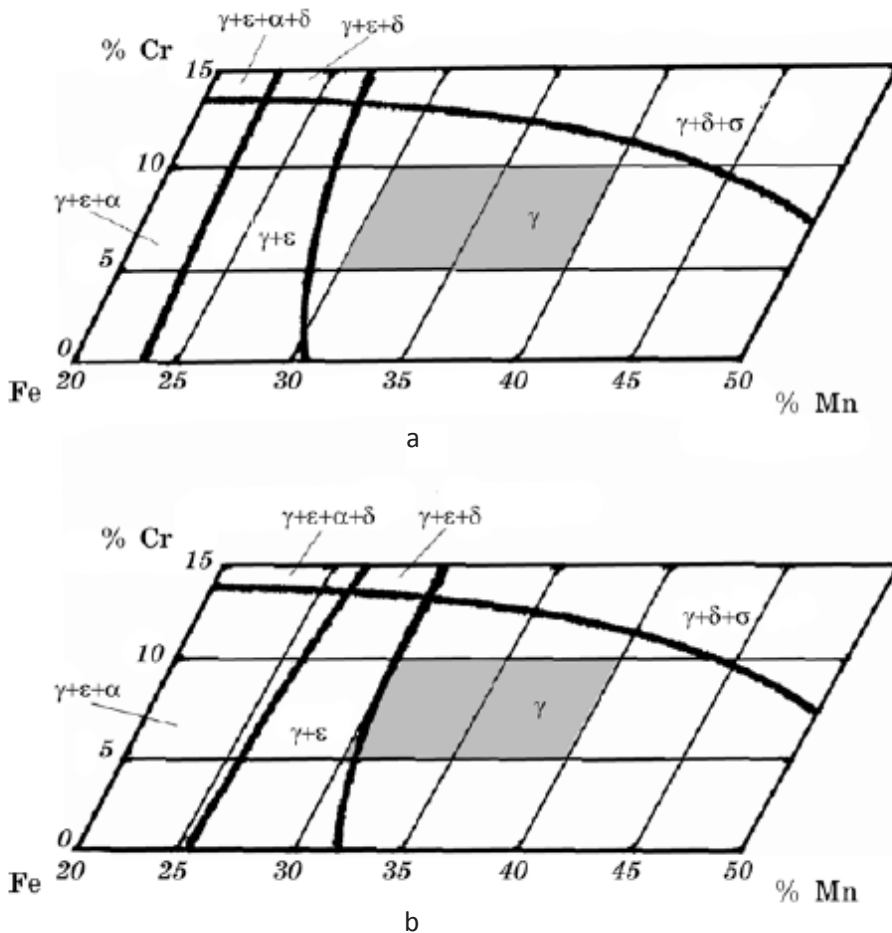

Fig. 1. Structural-phase diagrams of the Fe–Cr–Mn alloys according to the data in [4]: a) at 20 K, b) at 20 K after plastic deformation to fracture at the same temperature. The α-manganese ferrite (BCC-martensite), γ-austenite (FCC); ε-martensite (HCP); δ-ferrite (BCC); σ-chemical compound FeCr (the elementary cell is tetragonal and consists of 30 atoms of the type of β-uranium [7, 8]). The crosshatched area is the region of the concentration corresponding to the alloys investigated in the present study.

2.1. Resistance measurements

Resistance measurements were taken at direct current by the standard four-probe method. The current contacts were brazed to the ends of the specimens using a lead–tin brazing alloy. The potential contacts were welded to the specimens. The specimens were placed in a measuring cell in the direction normal to the axis of the electric heater in order to minimise the temperature gradient along the specimens. Measurements were taken at a transport current of 20 mA, the power scattering on the specimen did not exceed $8 \cdot 10^{-6}$ W. To exclude the effect of parasitic electromotive forces, measurements were taken at two opposite directions of the transport current.

2.2. Acoustic measurements

Acoustic measurements were taken using two resonance methods of mechanical spectroscopy: 1) the method of the double compound vibrator (the frequency of longitudinal oscillation $\cong 75$ kHz in the amplitude-dependent region of ultrasonic deformation $\varepsilon_0 \cong 10^{-7}$); 2) the method of bending oscillations with the electrostatic excitation of a free specimen at a frequency of $\cong 3$ kHz.

Nondestructive mechanical spectroscopy combines high structural sensitivity, selectivity and accuracy.

3. Measurements results and discussion

The resultant experimental data can be divided into two groups with each group relating to the specimens with the fixed content of Cr: 5 and 10%, respectively. The measured dependences inside each group have the form of general relationships discussed below.

3.1. Results of resistance measurements

The investigated alloys are characterised by a high residual electric resistivity $\rho(T = 0 \text{ K}) \approx 50–70$ µohm · cm. In the specimens with 5% Cr the value of ρ increases systematically with the increase of the manganese concentration. In the alloys with 10% chromium there is no systematic variation of ρ with the variation of the concentration of manganese and iron (Fig. 2).

3.2. Results of acoustic measurements

Figures 3 and 4 show the temperature dependences of the logarithmic decrement of oscillations $\delta(T)$ and the dynamic Young modulus $E(T)$, measured in the temperature range 5–325 K. The investigated alloys are characterised by the relatively low values of $\delta < 6 \cdot 10^{-4}$ and a high value of $E \cong 180$ GPa which
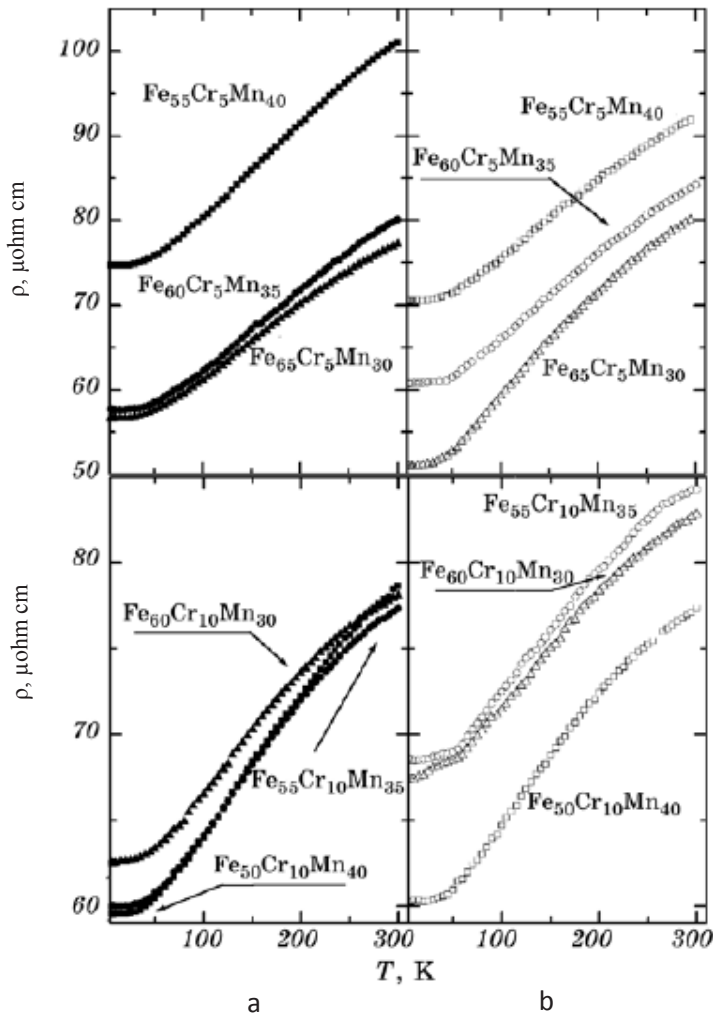
Fig. 2. Temperature dependences of specific electrical resistivity of Fe95–xCr5Mn and Fe9–xCr10Mnx alloys: a) thick specimens, b) wire specimen.

monotonically increases by 7% with the temperature decreasing from 325 to 5 K. In the wire specimens the value δ is 2–3 times higher and the value of E is 5–10% lower in comparison with a stick specimens. A possible reason for these differences may be the difference in the structure of the wire and thick specimens.

The dependence $\delta(T)$ for the alloys with 5% Cr showed a series of peaks P_1 (≈20 K), P_2 (≈155K) and P_3 (≈ 255K). The height of the peak P_1 decreases with increasing manganese concentration, and the peak transforms into a plateau. The parameters of the peaks P_2 and P_3 change only slightly and in a non-symmetric manner.

In the specimens with the chromium content of 10%, the $\delta(T)$ dependence

also shows internal friction peaks at $T_{P2} \approx 140$ K and $T_{P3} \approx 220$ K. The largest height of the peaks is recorded in the specimens with 40% Mn, the smallest in the specimens with 35% Mn. In the specimen with 5% Cr the peaks P_2 and P_3 are characterised by the complicated form and consists of two or more peaks. The peaks P_1, P_2 and P_3 have the frequency-dependent form – with the increase of the frequency of mechanical oscillations of the specimen the temperature at which the peaks form is displaced the two higher temperatures, indicating that the peaks formed by a thermally activated mechanism. However, the nature of these peaks has not as yet been investigated.

When the temperature is increased, the background absorption δ_{BG} increases quite rapidly. Taking into account the high temperature dependence of background absorption, it may be concluded that the absorption is caused partially by the non-conservative viscous movement of the dislocations [5] with the activation energy U_{BG}:

$$\delta_{BG} = A_1 + A_2 \exp\left(-\frac{U_{BG}}{kT}\right). \tag{1}$$

The coefficients A_1, A_2 and the diameter U_{BG} are fitting parameters and their values change with the change of the defective structure of the specimen. At the values A_1, A_2 and U_{BG}, presented in Table 1, the graphs of the function (1) for the investigated specimens are shown in Fig. 3a, c and Fig. 4a, by the solid lines.

The temperature dependence of the elasticity modulus $M(T)$ of simple crystalline materials in a wide temperature range is explained assuming the additive contribution of the electronic and phonon components [6]. In the temperature range $T \leq \Theta_D$ the dependence $M(T)$ is described with sufficient accuracy by the following relationship:

$$M(T) = M_0^{AD} - M_1 f\left(\frac{T}{\Theta_D}\right) - M_2 T^2, \tag{2}$$

where M_0^{AD} is the adiabatic modulus of elasticity of the ideal crystal at

$T \to 0$ K; $M_1 f\left(\dfrac{T}{\Theta_D}\right)$ is the defect of the modulus determined by the phonons;

$M_2 T^2$ is the defect of the modulus determined by the thermal motion of the conduction electrons:

$$f\left(\frac{T}{\Theta_D}\right) = \left(\frac{T}{\Theta_D}\right)^4 \int_0^{\frac{\Theta_D}{T}} dx \frac{x^3}{e^x - 1}$$

and Θ_D is the Debye temperature.

The solid lines in Fig. 3b, d and 4b, d indicate the theoretical temperature dependences of the elasticity modulus, calculated using the equation (2) at the values of the theoretical parameters presented in Table 1. It may be seen that
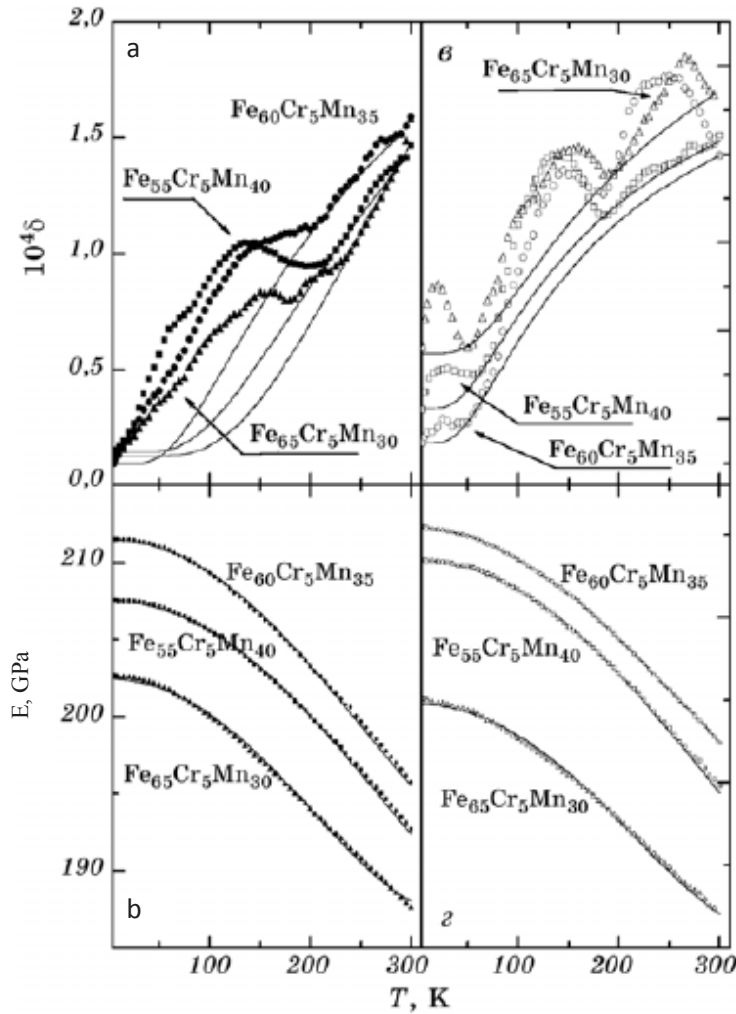
Fig. 3. Temperature dependences of the logarithmic decrement of oscillations (T) – (a, c) and the dynamic Young modulus $E(T)$ – b, d) in $Fe_{95-x}Cr_5Mn_x$ alloys: (a, b) – thick specimens, (c, d) – wire specimens. The solid lines in the figures (a, c) are the theoretical dependences of the background of acoustic absorption, calculated from equation (1); (b, d) are the theoretical temperature dependences of the elasticity modulus, calculated from equation (2).

the behaviour of the temperature dependence of the elasticity modulus, detected in the experiments, was described in detail in the model proposed in (2).

The increase of the Cr concentration at the constant manganese concentration in both the wire and thick specimens increases the parameter M_0^{AD}. This is in agreement with the data on the concentration dependence of the yield limit [3, 4]. The variation of the manganese concentration has a non-systematic effect on the absolute value of E and almost no effect on the form of the dependences $E(T)$.
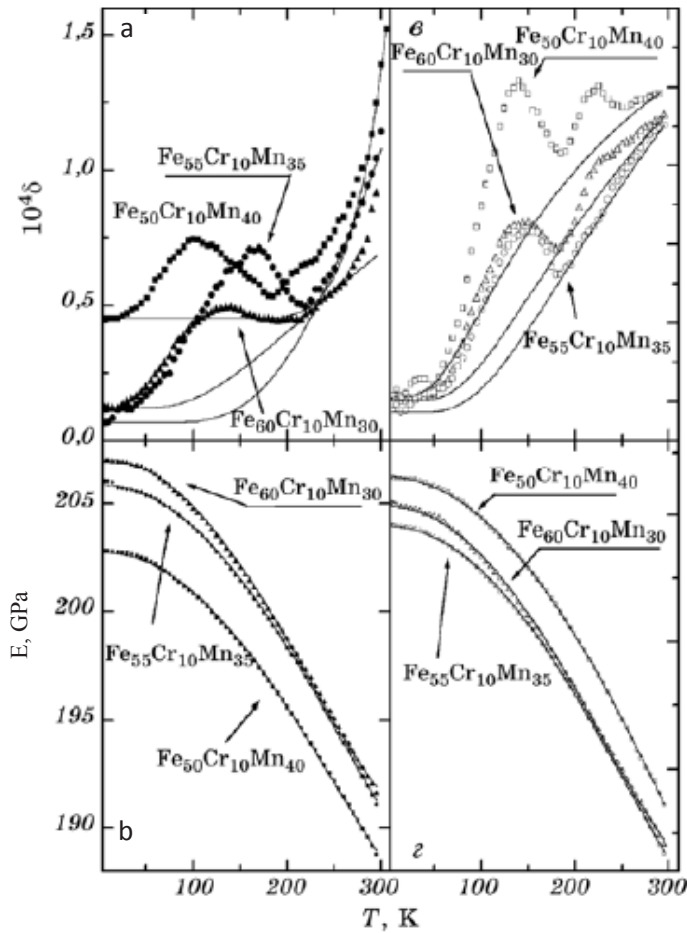
Fig. 4. Temperature dependences of the logarithmic decrement of oscillations δ(T) – (a, c) and the dynamic Young modulus $E(T)$ – b, d) in $Fe_{90-x}Cr_{10}Mn_x$ alloys: (a, b) – thick specimens, (c, d) – wire specimens. The solid lines in the figures (a, c) are the theoretical dependences of the background of acoustic absorption, calculated from equation (1); (b, d) are the theoretical temperature dependences of the elasticity modulus, calculated from equation (2).

4. Conclusion

It is well-known that the γ↔ε transformation is accompanied by a sudden jump of the value of ρ and by the appearance of the absorption peak. The temperatures of the direct and reversed transformations do not coincide, and a hysteresis loop is detected in the temperature dependences ρ(T) and $E(T)$. The dependences recorded in this study do not show these special features and this indicates that the structure of the investigated alloys was stable in the investigated temperature range. However, the non-systematic variation of the acoustic and resistivity properties detected for the alloys with 10% chromium may be associated with

Table 1. Empirical parameters of the temperature dependence of the background of acoustic absorption and elasticity modulus in the thick (wire) specimens of chromium–manganese steels

Cr concentration	5%			10%		
Mn concentration	30%	35%	40%	30%	35%	40%
$A_1 \cdot 10^5$	1.0 (17)	0.9 (7)	1.4 (11)	1.2 (10)	0.7 (9)	4.9 (11)
$A_3 \cdot 10^4$	7.5 (5.1)	3.2 (5.5)	4.3 (6.0)	2.4 (10.3)	17.6 (13.3)	6.1 (7.4)
U_{BG}, eV	0.044	0.020	0.031	0.037	0.074	0.023
	(0.014)	(0.013)	(0.018)	(0.027)	(0.032)	(0.016)
M_0^{AD}, GPa	203 (185)	212 (196)	208 (194)	207 (196)	206 (195)	203 (197)
M_1, MPa · K⁻⁴	74 (57)	40 (31)	28 (19)	59 (46)	35 (30)	34 (10)
M_2, MPa · K⁻²	1569	1225	1165	1137	1001	981 (985)
	(950)	(759)	(866)	(1080)	(1026)	
	427 (416)	419 (404)	409 (402)	448 (422)	445 (412)	440 (403)

small inclusions of the ε-martensite phase, formed in the process of preparation of the specimen. The presence of this phase has been confirmed by x-ray diffraction examination. A structural factor should also be considered: supersaturation of the alloy with manganese and the formation of large clusters with long-range ordering.

References

1. E. S. Kagan, et al., MiTOM, No. 10, 18 (1971).
2. Ya. V. TRantsevich, te al., Probl. Prochn., No. 10, 97 (1971).
3. G. Grikurov, et al., J. Phys. IV, 112, 279 (2003).
4. G.Grikurov, et al., Adv. Cryog., 50 (2004).
5. V.S. Postnikov, Internal friction in Metals, Metallurgizdat, Moscow, 1974.
6. H. Leybfried, Microscopic theory of mechanical and themal properties of crystals, Fizmatgiz, Moscow, 1963.
7. M. Hansen and K. Anderko, Structure of binary alloys, Metallurgizdat, Moscow, 1962.
8. F.N. Tavadze (editor), Metallography of iron, Metallurgizdat, Moscow, 1972.